

PACS numbers: 42.55.Lt; 42.55.Rz; 42.60.By; 42.65.Jx; 42.65.Ky; 52.50.Jm
DOI: 10.1070/QE2013v043n040ABEH015140

Production of extended plasma channels in atmospheric air by amplitude-modulated UV radiation of GARPUN-MTW Ti:sapphire–KrF laser. Part 1. Regenerative amplification of subpicosecond pulses in a wide-aperture electron beam pumped KrF amplifier

V.D. Zvorykin, A.A. Ionin, A.O. Levchenko, G.A. Mesyats, L.V. Seleznev, D.V. Sinitsyn, I.V. Smetanin, E.A. Sunchugasheva, N.N. Ustinovskii, A.V. Shutov

Abstract. **Regenerative amplification of single and multiple ultrashort subpicosecond UV pulses in a wide-aperture KrF amplifier with an unstable confocal resonator was investigated on the GARPUN-MTW hybrid laser system. Amplitude-modulated 100-ns long UV radiation pulses with an energy of several tens of joules were obtained at the output of the system. The pulses were a combination of a quasi-stationary oscillation pulse and a train of amplified ultrashort pulses (USPs) with a peak power of 0.2–0.3 TW, which exceeded the power of free-running lasing pulse by three orders of magnitude. The population inversion recovery time in the active KrF laser medium was estimated: $\tau_c \leqslant 2.0$ ns. Trains of USPs spaced at an interval $\Delta t \approx \tau_c$ were shown to exhibit the highest amplification efficiency. The production of amplitude-modulated UV pulses opens up the way to the production and maintenance of extended plasma channels in atmospheric air.**

Keywords: *plasma channels, ultrashort laser pulses, KrF laser, train of ultrashort pulses.*

1. Introduction

The possibility of producing with the help of laser radiation an extended (tens and hundreds of metres in length) conducting plasma channel in the atmospheric air has attracted the attention of researchers since the 1970s. An artificial plasma waveguide may be employed for wireless transmission of electric current [1, 2] as well as of microwave and radio-frequency electromagnetic radiation for lowering its natural divergence [3–7]. Among important practical problems are the development of an active lightning protection system involving laser initiation and lightning trajectory control (see, for instance, papers [8–13] and references therein) as well as remote monitoring of atmospheric pollution with the use of a nitrogen laser operating in the regime of single-pass radiation amplification in the plasma channel produced by high-power ultrashort pulses (USPs) in the air [14]. Of special interest for the solution of these problems is UV laser radiation, for which the multiphoton ionisation probability of the air is considerably higher than for IR radiation [15], and it becomes the main gas ionisation mechanism even for relatively low radiation intensities $I \geqslant 5 \times 10^8$ W cm^{-2} readily attainable with laser pulses tens or hundreds of nanoseconds in duration. This is attested, for instance, by the experiments of Refs [7, 13], where the 100-ns long UV pulses of GARPUN KrF laser radiation produced hollow plasma waveguides, which transmitted microwave radiation for a distance tens of metres in length, and by extended plasma channels, which efficiently controlled a high-voltage discharge approximately 1 m in length. When the radiation of an electric-discharge KrF master oscillator was injected into the unstable confocal resonator, the output laser energy amounted to 100 J and the divergence of the UV radiation (λ = 248 nm) was equal to $\sim 2 \times 10^{-4}$ rad [16]. On equipping the laser with a femtosecond Ti:sapphire starting complex, the new GARPUN-MTW Ti:sapphire–KrF hybrid laser system [17] acquired the capability to amplify subpicosecond pulses to an energy of ~1 J [18, 19], in addition to the capability of generating long (100 ns) UV pulses.

The background to the present work was formed by the experiments involving electron density measurements in the plasma produced by the radiation of the KrF master oscillator with a pulse duration τ = 25 ns [7], which highlighted two significant circumstances. First, for intensities $I \geqslant 3 \times 10^8$ W cm^{-2} the photoelectron density n_e increases quadratically with intensity: $n_e \backsim I^2$. This takes place in accord with the stepwise three-photon ionisation mechanism (2 + 1), Resonance Enhanced Multiphoton Ionisation (REMI), of oxygen molecules [20], which have the lowest ionisation potential among the air components (I_i = 12.06 eV). Second, in the sequential action of two laser pulses spaced at a period approximately equal to the electron lifetime ($\Delta t \approx \tau_e$), not only does the second pulse produce its own portion of photoelectrons, but it also detaches those which were produced by the first pulse and managed to adhere to O_2 molecules. In this case, a relatively low radiation intensity (~10^7 W cm^{-2}) is required for the efficient photodetachment of the adherent electrons [7]. Therefore, by going over from a smooth 100-ns long UV pulse to a combined amplitude-modulated pulse consisting of a USP train and a long pulse of quasi-stationary lasing, with the GARPUN-MTW facility it will be possible to

V.D. Zvorykin, A.A. Ionin, A.O. Levchenko, G.A. Mesyats, L.V. Seleznev, D.V. Sinitsyn, I.V. Smetanin, E.A. Sunchugasheva, N.N. Ustinovskii, A.V. Shutov P.N. Lebedev Physics Institute, Russian Academy of Sciences, Leninsky prosp. 53, 119991 Moscow, Russia; e-mail: zvorykin@sci.lebedev.ru

Received 30 January 2013; revision recieved 12 February 2013
Kvantovaya Elektronika **43** (4) 332–338 (2013)
Translated by E.N. Ragozin

substantially increase the electron plasma density [21–24]. This proposal was realised in our primary experiments [25, 26].

The first part of the present work is concerned with a detailed description of the scheme and lasing dynamics of amplitude-modulated high-energy 100-ns long UV laser pulses in the regime of regenerative amplification of a train of subpicosecond pulses in a wide-aperture KrF amplifier with electron-beam pumping. The second part demonstrates the advantages of amplitude-modulated pulses in the production of extended plasma channels in the atmosphere and the control of high-voltage electric discharges [27].

2. Analysis of short pulse train amplification in KrF amplifiers

Among the distinctive features of the active medium of a KrF $B \to X$ transition laser are high values of the cross section for stimulated emission, $\sigma = 2.5 \times 10^{-16}$ cm^2, and of the small-signal gain g_0, the short lifetime $\tau_c \approx 2$ ns of the excited state (equal to the population inversion recovery time in the quasi-stationary case) determined by the high spontaneous emission probability from this state and fast collisional quenching, as well as a rather large nonsaturable absorption coefficient α_{ns} for laser radiation due to excited components of the working mixture at typical pressures of 1–2 atm [28]. For a specific excitation power $W \approx 1$ MW cm^{-3} typical for electron-beam pumped lasers with a large active volume, the gain g_0 and absorption α_{ns} coefficients are proportional to W and their ratio ($g_0/\alpha_{ns} = 10–20$) varies only slightly under variation of the pump intensity [28].

The incoherent amplification of a USP with a duration $\tau \ll \tau_c$ is described by the modified Frantz–Nodvik equation [29]:

$$\frac{d\varepsilon}{dx} = g(x)(1 - e^{-\varepsilon}) - \alpha_{ns}\varepsilon, \quad (1)$$

where $\varepsilon = Q/Q_s$;

$$Q(x) = \int_0^\tau I(x,t')\,dt'$$

and $I(x,t)$ are the energy density and intensity of the USP in its propagation through the amplifier; $Q_s = h\nu/\sigma = 2$ mJ cm^{-2} is the saturation energy density; and $h\nu = 5$ eV is the laser photon energy. The profile of the gain $g(x)$ is formed by amplified spontaneous emission (ASE) [19] or by a long laser pulse amplified simultaneously with the USP [17, 30].

The local efficiency η_{1ext} of energy extraction from the active medium by a short laser pulse is defined as the ratio between the energy density increment in a unit amplifier length $dQ/dx = Q_s d\varepsilon/dx$ and the energy $N^* h\nu = (g_0/\sigma)h\nu = g_0 Q_s$ stored in the upper laser level (N^* is the density of KrF molecules excited to this level). In view of Eqn (1) we obtain the following expression for the local energy extraction efficiency along the amplifier:

$$\eta_{1ext}(x) = \frac{1}{g_0}[g(x)(1 - e^{-\varepsilon}) - \alpha_{ns}\varepsilon]. \quad (2)$$

Its highest value

$$(\eta_{1ext})_{max} = \frac{g}{g_0}\left[1 - \frac{\alpha_{ns}}{g}\left(1 + \ln\frac{g}{\alpha_{ns}}\right)\right] \quad (3)$$

is achieved for a relative energy density $\varepsilon_{opt} = \ln(g/\alpha_{ns})$.

The average efficiency of energy extraction from an amplifier of length L is defined by the formula

$$\langle\eta_{1ext}\rangle = \frac{1}{L}\int_0^L \eta_{1ext}(x)\,dx = \frac{\varepsilon(L) - \varepsilon(0)}{g_0 L}. \quad (4)$$

To estimate the characteristic efficiency values, in the simplest case we put $g(x) \equiv g_0$ to obtain from expression (3) the highest efficiency of energy extraction by a single pulse $\eta_{1ext} = 1 - (\alpha_{ns}/g_0)[1 + \ln(g_0/\alpha_{ns})] = 0.67–0.8$ for the optimal USP energy density $Q_{opt} = Q_s \ln(g_0/\alpha_{ns}) = 4.6–6.0$ mJ cm^{-2}. To find the USP amplification efficiency relative to the pump energy, we must take into consideration that a single USP extracts the energy of active medium excitation stored for a period $\tau_c \approx 2$ ns, which is short in comparison with the characteristic duration of electron beam pumping $\tau_p \approx 100$ ns, and that the excitation efficiency of the upper laser level of KrF molecules relative to the specific pump power

$$\eta_p = \frac{N^* h\nu}{W\tau_c} = \frac{g_0 Q_s}{W\tau_c} = \frac{g_0 I_s}{W} \approx 0.25,$$

where $I_s = Q_s/\tau_c \approx 1$ MW cm^{-2} is the saturation intensity for the quasi-stationary amplification of long pulses ($\tau > \tau_c$). We arrive at the result that the single USP amplification efficiency relative to the pump energy (i.e. the electrooptical or internal amplifier efficiency), $\eta_1 = (\tau_c/\tau_p)\,\eta_{1ext}\eta_p \approx 0.004$, is low in comparison with the efficiency $\eta_{long} = 0.12$ of quasi-stationary long pulse amplification [28, 30].

Since the accumulation of excited KrF molecules on the upper laser level is impossible for $\tau_c \ll \tau_p$, efficient energy extraction should be effected using a train of pulses spaced at a period Δt approximately equal to the lifetime of the excited state ($\Delta t \approx \tau_c$). In this case, the gain for each of the subsequent pulses is saturated by the preceding pulses and turns out to be lower than in the amplification of a single USP [30, 31]:

$$g_{\Delta t} = g_0 \frac{1 - \exp(-\Delta t/\tau_c)}{1 - \exp(-\varepsilon)\exp(-\Delta t/\tau_c)}. \quad (5)$$

For an energy density

$$Q_{opt} = Q_s \ln\{2\exp(-\Delta t/\tau_c) + (g_0/\alpha_{ns})[1 - \exp(-\Delta t/\tau_c)]^2\}$$

the efficiency of USP train amplification is highest:

$$\eta_{ext} = \frac{1}{\Delta t/\tau_c}\left\{\frac{[1 - \exp(-\Delta t/\tau_c)][1 - \exp(-\varepsilon_{opt})]}{1 - \exp(-\varepsilon_{opt})\exp(-\Delta t/\tau_c)} - \frac{\alpha_{ns}\varepsilon_{opt}}{g_0}\right\}. \quad (6)$$

For a pulse sequence interval $\Delta t \approx \tau_c = 2$ ns and $Q_{opt} = 3.1–4.3$ mJ cm^{-2} we obtain $\eta_{ext} = 0.38–0.48$. In this case, the USP train amplification efficiency $\eta_{train} = \eta_{ext}\eta_p = 0.095–0.12$ relative to the pump is comparable to the efficiency of long pulse amplification.

The amplification of single USPs in a long double-pass amplifier proceeds under conditions of a quasi-stationary profile of the gain $g(x)$ saturated by ASE [19]. As a consequence, the energy and efficiency of USP amplification will be somewhat lower than in the case $g(x) \equiv g$ considered above. A similar picture will also take place for the regenerative multiple-pass amplification of a single USP in the resonator, where the developing quasi-stationary oscillation extracts from the active medium the greater part of the energy restored by pumping. However, in the amplification of a USP train one would expect that the USPs will have an advantage due to their high peak power, provided that the short-pulse sequence interval will be shorter that the characteristic settling time of quasi-stationary oscillation. By the order of magnitude, this is

the resonator round trip time $\tau_{osc} \approx 2L_{res}/c$, which was equal to ~17 ns for the unstable resonator of length $L_{res} = 2.5$ m in the present work.

3. Facility description

In the regenerative amplification of the trains of subpicosecond pulses in the final KrF amplifier of the GARPUN-MTW laser facility, in the present work we made use of the same laser elements as in the previous experiments on the double-pass amplification of single USPs [18, 19]; however, they were arranged in a different way (Fig. 1). The Ti:sapphire Start-248M (Avesta Project Ltd.) starting complex with radiation frequency conversion to the third harmonic generated USPs with a duration of about 100 fs, an energy of up to 0.5 mJ, and a wavelength $\lambda = 248.4$ nm tuned to the peak of the B → X KrF amplification band. In the alignment of the amplification path and recording instrumentation, the starting complex was operated at repetition rate of 10 Hz; in the operating regime, a single USP timed to the pumping of KrF amplifiers was gated using an electromechanical shutter. In this case, the output beam 8 mm in diameter was transmitted through a vacuum spatial filter (not shown in Fig. 1), where it was telescoped with a three-fold magnification to reduce the nonlinear distortions in the long aerial path approximately 50 m in length. Then, the single USP was fed to the ring pulse multiplication circuit comprising plane mirrors: three totally reflecting mirrors and a semi-transparent one M1 with a reflection coefficient of 30% (Fig. 1). This circuit transformed the pulse to a sequence of equally spaced USPs with an amplitude ratio of 3:5:1.5: 0.5.... The directions of multiplied pulse propagation were brought into coincidence by aligning the mirrors, and their temporal spacing $\Delta t \approx 5.3$ ns was defined by the distance between the mirrors (by the circuit round trip time).

The USP train formed in this way was delivered to the input of a Berdysh KrF preamplifier with an active volume of $8 \times 8 \times 110$ cm pumped by an electron beam [17–19]. The specific pump power W of the Ar–Kr–F_2 working mixture pressurised to a pressure of 1.8 atm was equal to 0.6–0.7 MW cm^{-3}. The cross section of the laser beam was matched to the preamplifier aperture using convex M2 and concave M3 mirrors with dielectric coatings. Upon amplification in the double-pass amplifier the beam was focused onto the pinhole of a spatial filter. The diverging beam was next collimated with a lens and directed to the GARPUN final regenerative amplifier with an active volume of $12 \times 18 \times 100$ cm and a working mixture pressure of 1.4 atm, which was pumped by two counterpropagating electron beams with a specific pump power $W = 0.7$–0.8 MW cm^{-3} [17–19]. The FWHM pump duration was equal to ~100 ns for both amplifiers. The electron guns of the amplifiers were timed to the femtosecond starting complex using an electric discharge KrF master oscillator, whose pulse (150 mJ, 20 ns) actuated the laser-triggered gaps of five pulse-forming lines in the high-voltage feed system of the guns.

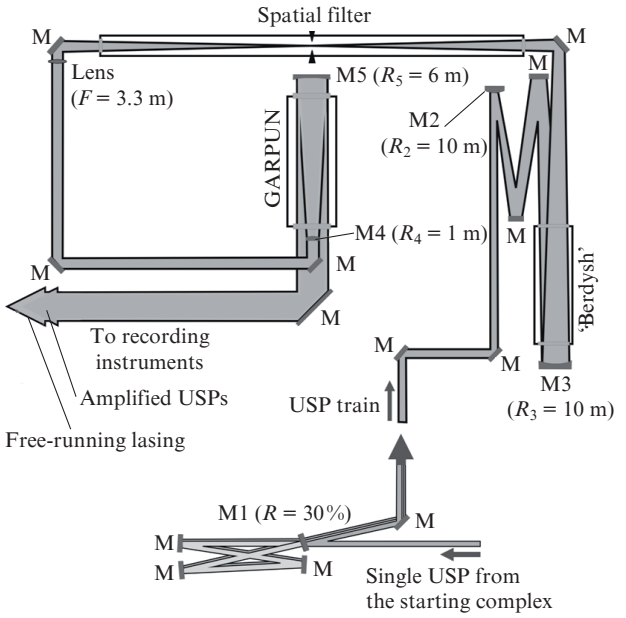

Figure 1. Schematic of experiments on the regenerative USP amplification in the GARPUN-MTW laser system.

The unstable confocal resonator of the GARPUN regenerative amplifier was formed by a totally reflecting spherical mirror M5 with a radius of curvature $R_5 = 6$ m and a semi-transparent mirror M4 deposited on the convex face of a meniscus lens with $R_4 = 1$ m. Therefore, the resonator magnification $M_{res} = R_5/R_4 = 6$ and length $L_{res} = (R_5 - R_4)/2 = 2.5$ m. The concave surface of the meniscus lens had an antireflection coating, and its radius of curvature was selected in such a way as to make coincident the points of the imaginary foci of the meniscus lens and the mirror deposited on the convex surface. The wavefronts of the beam injected into the resonator and the radiation reflected from the mirror surface of the meniscus lens in the multiple passes through the resonator were thereby matched to each other. A similar scheme for the injection of 20-ns long pulses of a KrF master oscillator into a resonator was employed in our earlier work [16], and when its power exceeded the ASE power it was possible to efficiently control the divergence and spectrum of the output radiation of the GARPUN laser.

All optical elements in the amplification path operating in transmission mode (i.e., the amplifier and interstage spatial filter windows, the lenses of the spatial filter placed after the starting complex, the collimating and meniscus lenses of the unstable resonator, as well as semi-transparent mirror M1 in the ring circuit) were made of high-purity FKU-grade calcium fluoride, which possesses the lowest nonlinear absorption for the USP radiation at $\lambda = 248$ nm [32, 33]. We emphasise that the wide-aperture KrF amplifier windows, unlike the rest of transmission optical elements, were made not of single crystals, but of randomly oriented crystalline aggregates, which was responsible for large-scale spatial nonuniformities in the distribution of amplified radiation intensity [18, 19].

4. Regenerative amplification of subpicosecond pulses

The Berdysh preamplifier was operated in the regime of unsaturated amplification and provided in two passes an amplification factor $G \approx 70$ and an output USP train energy of ~20 mJ for an aperture filling factor of ~60%. Figure 2 shows the characteristic signals of the radiation amplified in the preamplifier after passage through the spatial filter. The time in the oscilloscope traces is counted from the instant of triggering of the oscilloscope sweep. Shown for comparison on the same scale (i.e., for the same oscilloscope sensitivity)

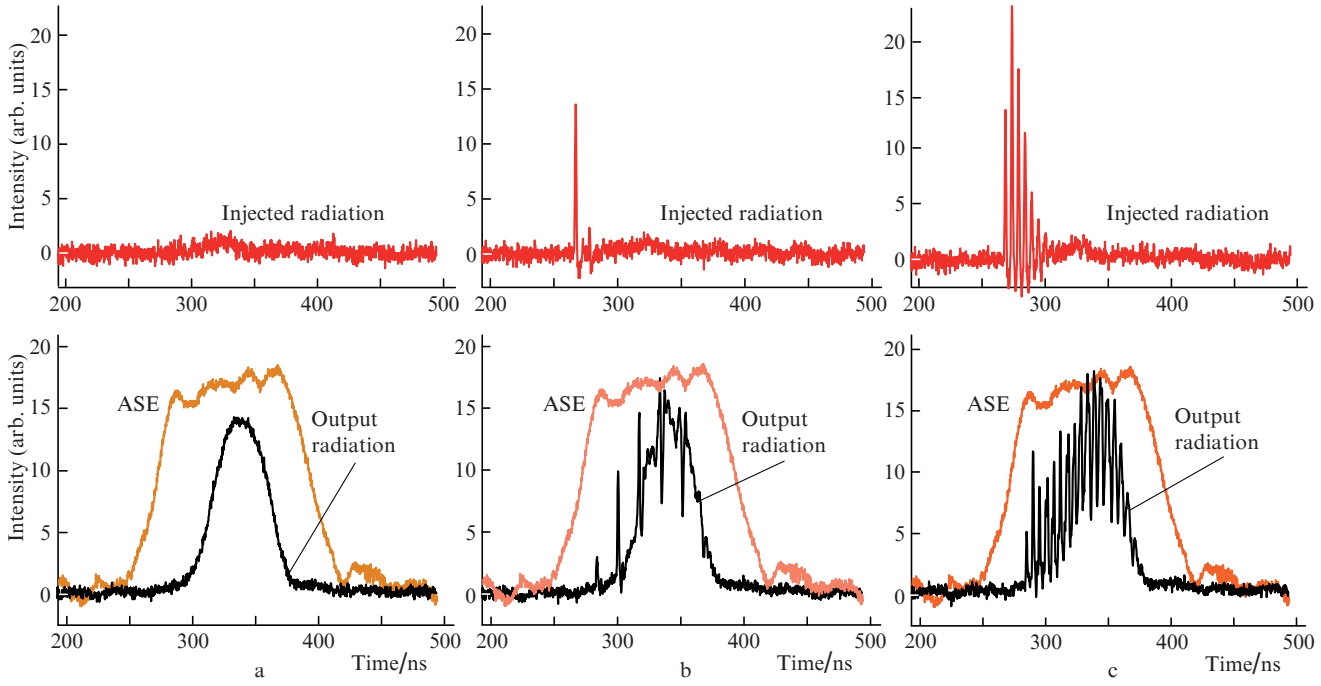

Figure 2. Oscilloscope traces of the radiation injected into the resonator (above) as well as of output radiation pulses and ASE in the transverse direction (below) in the case of free-running lasing (a), in the injection of a single USP into the resonator (b), and in the injection of a USP train (c). The vertical scale for (a), (b) and (c) is the same; the USP amplitude in the oscilloscope traces (b) and (c) is lowered 1000-fold because of the insufficiently high temporal resolution of the photodetector.

are the oscilloscope traces obtained in the absence of USPs at the preamplifier input, the oscilloscope traces of a single amplified USP when the multiplication channel was shut off, and of the amplified USP train. The signals were recorder using a FEK 29 KPU coaxial vacuum photodetector with a temporal resolution of ~1 ns, which was illuminated by the strongly attenuated radiation transmitted through the deflecting mirror after the spatial filter (this and other photoddetectors employed are not shown in Fig. 1). According to the data of our previous experiments with the use of a streak camera, the duration of amplified USPs was shorter than 1 ps [18, 19], and therefore the photodetector integrated the signals and lowered the true USP amplitude by at least a factor of 1000. Another similar photodetector placed behind the deflecting mirror at the output of the laser system recorded the radiation of the regenerative amplifier. The typical signals at the amplifier output with the use of a meniscus lens M4 with a reflection coefficient R_{men} = 30% are shown on the same scale in Fig. 2. Also shown in Fig. 2 are the oscilloscope traces of spontaneous emission amplified over a length of 12 cm in the transverse direction to the optical axis of the GARPUN amplifier and measured with the third photodetector through the side window in the laser chamber. The amplitude of ASE in the transverse direction was much lower than the signals of output radiation. The signals from all photodetectors were recorded with a Tektronix TDS-3054 four-channel oscilloscope with a sampling frequency of 5 GHz.

As is evident from the oscilloscope traces depicted in Fig. 2a, in the absence of an USP at the input of the preamplifier the ASE signal after the spatial filter is at a level of photodetector noise. In this case, the radiation pulse at the output of the GARPUN final stage is the oscillation pulse developing in the resonator from spontaneous emission with a delay relative to the pump pulse. On shutting off the resonator input the output signal was hardly changed, i.e. the spatial filter efficiently decoupled the amplifying stages as regards ASE. Depending on the meniscus lens reflection coefficient R_{men}, which was varied from 4% to 80% in our experiments (Table 1), the lasing pulse delay varied from 30 to 50 ns, which corresponds approximately to two or three resonator round trip times. The FWHM duration of the laser pulse was equal to 70–80 ns; in view of the delay, this corresponds approximately to the pump pulse duration. Simultaneously with the development of lasing we observed saturation of the transverse ASE signal caused by the saturation of the gain in the active medium. A fraction of the output radiation reflected from a wedge plate was diverted to a calorimeter, which measured the output laser energy. The results of measurements are collected in Table 1. A maximum energy of 25 J was obtained for the meniscus lens with the highest reflection coefficient R_{men} = 80%. We emphasise that in our experiments, which were carried out with an external unstable resonator, a significant effect on the output laser energy was exerted by high Fresnel radiation loss from the amplifier windows, which had no antireflection coatings, as well as by the long-lived absorption induced in the windows by the X-ray bremsstrahlung of pump electron beams, which was accumulated in the course of long-term facility operation [34]. In view

Table 1. Energy of the laser radiation of the GARPUN module in relation to the reflection coefficient of the resonator meniscus lens.

R_{men} (%)	Radiation energy/J
4	10
10	15
30	15
80	25

of nontotal radiation reflection from the rear mirror M5 and meniscus mirror M4, this loss exceeded 60% in one round trip through the resonator, while the radiation fraction reflected from the meniscus mirror back into the unstable resonator (the resonator coupling constant) was equal to only $R_{men}(1/M_{res}^2) = 0.1\%-2.2\%$ for the meniscus mirrors with different reflection coefficients. Under these conditions the lasing energy turned out to be several times lower than in earlier experiments [16].

When a single USP was injected into the resonator of the GARPUN amplifier (Fig. 2b), it started circulating in the resonator and was amplified in the regenerative regime to compete with quasi-stationary lasing. The USP amplitude rises at the leading edge of the pump pulse as the gain in the active medium becomes higher. In the subsequent passages the USP amplitude becomes lower due to gain saturation by the laser pulse. The USP in its turn also saturates the gain, which manifests itself in a sharp decrease in lasing power immediately after the USP. The dips become deeper with increase in the power of quasi-continuous lasing. We note that this effect is unnoticeable in the pulse of transverse ASE because of the short amplification length. Another reason for the gradual lowering of USP amplitude may lie with the insufficiently precise radiation injection relative to the resonator axis or with misalignment of the output meniscus mirror of the resonator: in multiple passages the amplified radiation will deviate progressively further from the optical resonator axis and depart from the sensitive area of the photodetector placed in the near-field region of output radiation. The misalignment effect was borne out in experiments in which the photodetector was placed in the far-field region behind an aperture stop located at the focus of a spherical mirror with a focal length $F = 8$ m. A small misalignment of the resonator had the effect that the photodetector recorded only one USP after the first passage through the resonator, while the subsequent USPs were completely rejected by the aperture stop. In this case, however, we recorded dips in the quasi-stationary lasing related to USP amplification. We note that for a strong misalignment of the meniscus mirror the regenerative amplifier actually turned into a double-pass amplifier and produced only one amplified USP in the absence of quasi-stationary lasing.

When a USP train with a pulse separation $\Delta t \approx 5.3$ ns was injected into the resonator (Fig. 2c), the output radiation was a superposition of different pulses of the train amplified in multiple passages through the resonator, which partly suppressed the quasi-stationary lasing. The output was a strongly modulated pulse with an overall duration of 100 ns and a very high radiation power in individual peaks, which was more than 1000 times higher than the power of quasi-stationary lasing.

Measurements of the output radiation energy showed that it was the same both in the regime of free-running lasing and in the injection of a single USP or a USP train into the resonator, and depended only on the reflection coefficient of the meniscus mirror (see Table 1). The output pulse modulation depth also depended on the reflection coefficient. Although the highest energy was obtained for the most reflecting meniscus mirror with $R_{men} = 80\%$, the radiation modulation depth was relatively shallow. The optimal ratio between the energy of output radiation and its modulation depth was reached for more transparent meniscus mirrors with $R_{men} = 10\%$ and 30%, for which the energy was equal to 15 J. By comparing the oscilloscope traces in Figs 2a and 2c and considering that the quasi-stationary lasing energy is approximately equal to the energy contained in the train of 20 USPs in the case of combined pulse (i.e., that the corresponding areas under the oscilloscope traces in Figs 2a and 2c are equal) as well as assuming that the duration of the USPs is equal to ~1 ps, we estimate their peak power at 0.2–0.3 TW. In reality, owing to group velocity dispersion the duration of the USPs in the train increases monotonically for the subsequent pulses in multiple passages through the thick (~3 cm) amplifier windows. We also note that the energy of combined pulses generated by the GARPUN-MTW laser system may be increased several-fold by lowering the parasitic radiation loss in the resonator caused by the windows of the laser chamber of the regenerative amplifier.

5. Measurements of gain recovery time in the active medium of the KrF laser

Knowledge of the population inversion recovery time τ_c in the active medium of a KrF laser is significant not only for the realisation of efficient amplification of the train of USPs with duration $\tau \ll \tau_c$ (see Section 2), but also for the numerical simulation of large-scale KrF laser drivers for inertial confinement fusion (ICF) [35]. Angular beam multiplication [36], which is employed for the quasi-stationary amplification of a nanosecond pulse train in amplifiers with a long duration of electron beam pumping (100–500 ns), also permits combining nanosecond pulses and USPs to obtain a complex temporal radiation on-target profile [30, 37] required for prospective ICF schemes with separate compression and heating of the fuel [38, 39]. In numerical simulations it is usually assumed that $\tau_c \approx 2$ ns [28], although this quantity, apart from the radiative decay rates and quenching rates in collisions with components of the active medium mentioned above, also depends on the rate of vibrational relaxation of the upper electronic state of KrF molecules, i.e. the τ_c values may be considerably different in different theoretical models of vibrational kinetics. For instance, the value $\tau_c = 3$ ns calculated by A.G. Molchanov under a six-level semi-phenomenological model approximation [40, 41] turns out to be twice as high as the value obtained using a multilevel KrF laser model [37, 42, 43].

The investigation of the amplification dynamics performed in the present work for the active medium of a KrF amplifier, which was loaded simultaneously by quasi-stationary lasing and USPs, permits determining more precisely the τ_c value and thereby verify the adequacy of the theoretical models in use. Figure 3 shows different portions of the combined laser pulse when a single USP was injected into a slightly misaligned resonator. In the oscilloscope trace of the initial portion (Fig. 3a) one can see an USP amplified during the first passage through the resonator and broadened by the photodetector (peak 1); after the second passage its amplitude is several times smaller (peak 2) owing to the misalignment of the resonator (see Section 4). By contrast, the dips (I–III) in the pulse of quasi-stationary lasing, which are caused by saturation of the active medium of the KrF amplifier, are deeper. At a later stage, when the quasi-stationary lasing power reaches its maximum (Fig. 3b), the USPs are hardly discernible against its background, while the depth of the dips due to the USP circulating in the resonator remains approximately constant until the power of lasing begins to fall off. The points in the oscilloscope traces correspond to the frequency of signal digitisation and are spaced at 0.2 ns. From the oscilloscope traces one can see that the USP rise time of 1.0–1.2 ns is equal to the gain decrease time (the dip leading edge) and corresponds to the temporal resolution of the photodetector.

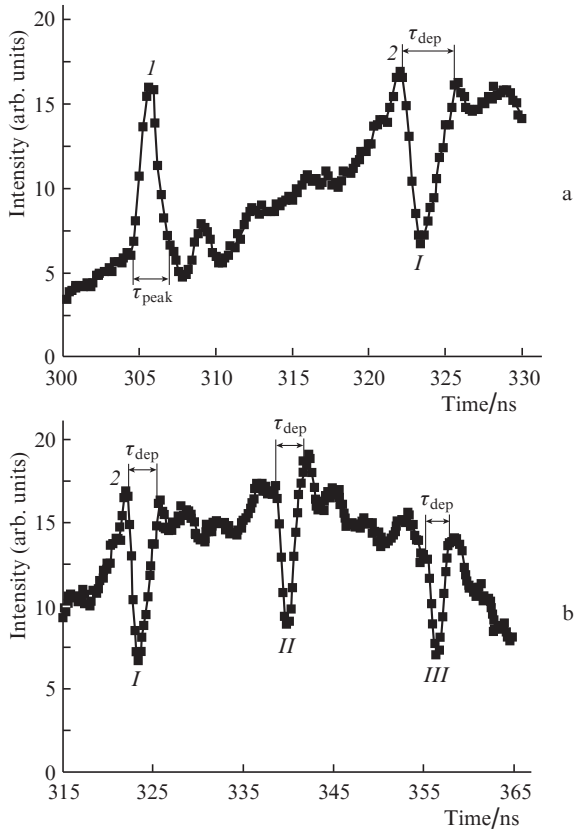

Figure 3. Oscilloscope traces of a combined laser pulse at the initial stage of gain build-up (a) and near the peak of quasi-stationary lasing power (b); τ_{peak} is the USP duration broadened by the photodetector, τ_{dep} is the period of quasi-stationary lasing decrease after the passage of a USP. Peaks *1* and *2* and dips *I*–*III* correspond to successive resonator passages by a single USP; the time in the oscilloscope traces is counted from the sweep start.

The recovery of gain after the USP proceeds in a longer time of 2.0 ± 0.2 ns; in view of the temporal photodetector resolution this an upper estimate for $\tau_c \leqslant 2.0$ ns. The τ_c value found in the present experiments is closer to the value calculated in the multilevel KrF laser model [37, 42, 43].

6. Conclusions

Regenerative amplification of single and multiple subpicosecond UV laser pulses in a wide-aperture KrF amplifier with electron-beam pumping was investigated on the GARPUN-MTW multistage hybrid laser system. The ultrashort pulses were generated by a titanium-sapphire starting complex, frequency-tripled, multiplied to a pulse train, and amplified in a double-pass KrF preamplifier to an energy of ~20 mJ. The train of amplified USPs, which were spaced at intervals of the order of population inversion recovery time in the active medium, was then injected into an unstable confocal resonator of the final regenerative KrF amplifier. Combined amplitude-modulated 100-ns long pulses with an energy of several tens of joules were obtained at the output of the laser system. These pulses were the superposition of the quasi-stationary lasing pulse and the USP train with a peak power of 0.2–0.3 TW, which was 1000 times higher than the power of free-running lasing in the absence of USP injection into the resonator. We found the population inversion recovery time $\tau_c \leqslant 2.0$ ns in the active KrF laser medium, which corresponds to the time calculated proceeding from the multilevel theoretical model of vibrational kinetics of the upper electronic state of KrF (B) molecules.

Acknowledgements. This work was supported by the programmes 'Extreme Light Fields and Their Applications' and 'Fundamental Problems of Pulsed High-Current Electronics' of the Presidium of the Russian Academy of Sciences, by the Russian Foundation for Basic Research (Grant Nos 11-02-01414, 11-02-01524, 11-02-12061-ofi-m, and 12-02-31431-mol_a) and by the EOARD (Grant No. 097007) in the framework of the ISTC Partner Project No. 4073 R.

References

1. Koopman D.V., Wilkenson T.D. *J. Appl. Phys*., **42**, 1883 (1971).
2. Zvorykin V.D., Nikolaev F.A., Kholin I.V., et al. *Fiz. Plazmy*, **5**, 1140 (1979).
3. Askar'yan G.A. *Zh. Eksp. Teor. Fiz*., **55**, 1400 (1968).
4. Chateauneuf M., Payeur S., Dubois J., Kieffer J.-C. *Appl. Phys. Lett.*, **92**, 091104 (2008).
5. Zvorykin V.D., Levchenko A.O., Ustinovskii N.N., Smetanin I.V. *Pis'ma Zh. Eksp. Teor. Fiz*., **91**, 224 (2010).
6. Valuev V.V., Dormidonov A.E., Kandidov V.P., et al. *Radiotekh. Elektron*., **55**, 222 (2010).
7. Zvorykin V.D., Levchenko A.O., Shutov A.V., et al. *Phys. Plasmas*, **19**, 033509 (2012).
8. Zhao X.M., Wang Y.C., Diels J.-C., Elizondo J. *IEEE J. Quantum Electron*., **31**, 599 (1995).
9. *Upravlenie razryadom molnii s pomoshch'yu lazernogo izlucheniya* (Control over Lightning Discharge by Laser Radiation) *Opt. Zh*., **66** (3) (1999).
10. Bazelyan E.M., Raizer Yu.P. *Fizika molnii i molniezashchita* (The Physics of Lightning and Lightning Protection) (Moscow: Fizmatlit, 2001).
11. Bazelyan E.M., Raizer Yu.P. *Usp. Fiz. Nauk*, **170**, 753 (2000) [*Phys. Usp*., **43** (7), 701 (2000)].
12. Kasparian J., Ackermann R., Andre Y.-B., et al. *Opt. Express*, **16**, 5757 (2008).
13. Zvorykin V.D., Levchenko A.O., Ustinovskii N.N. *Kvantovaya Elektron*., **41** (3), 227 (2011) [*Quantum Electron*., **41** (3), 227 (2011)].
14. Penano J., Sprangle P., Hafizi B., et al. *J. Appl. Phys*., **111**, 033105 (2012).
15. Couairon A., Berge L. *Phys. Rev. Lett*., **88**, 135003 (2002).
16. Basov N.G., Vadkovskii A.D., Zvorykin V.D., et al. *Kvantovaya Elektron*., **21** (1), 15 (1994) [*Quantum. Electron*., **24** (1), 13 (1994)].
17. Zvorykin V.D., Didenko N.V., Ionin A.A., et al. *Laser Part. Beams,* **25**, 435 (2007).
18. Zvorykin V.D., Ionin A.A., Levchenko A.O., et al. *J. Phys. Conf. Ser*., **244**, 032014 (2010).
19. Zvorykin V.D., Levchenko A.O., Ustinovskii N.N. *Kvantovaya Elektron*., **40** (5), 381 (2010) [*Quantum. Electron*., **40** (5), 381 (2010)].
20. Johnson P.M., Otis C.E. *Annu. Rev. Phys. Chem*., **323**, 139 (1981).
21. Zvorykin V.D., Levchenko A.O., Smetanin I.V., Ustinovskii N.N. Patent of the Russian Federation, No. 90620. Priority of 21.09.2009.
22. Zvorykin V.D., Levchenko A.O., Smetanin I.V., Ustinovskii N.N. Patent of the Russian Federation, No. 2406188. Priority of 15.09.2009.
23. Zvorykin V.D., Levchenko A.O., Smetanin I.V., Ustinovskii N.N. Patent of the Russian Federation, No. 2411662. Priority of 31.05.2010.
24. Zvorykin V.D., Levchenko A.O., Smetanin I.V., Ustinovskii N.N. *Trudy XIII Shkoly molodykh uchenykh 'Aktual'nye problemy fiziki' i IV Shkoly-seminara 'Innovatsionnye aspekty fundamental'nykh issledovanii'* (Proc. XIIIth School for Young Scientists 'Topical Physical Problems' and IVth Workshop 'Innovative Aspects of Basic Research') (Zvenigorod–Moscow, FIAN, 2010) p. 144.
25. Zvorykin V.D., Ionin A.A., Levchenko A.O., et al. *Tezisy dokladov 39 Mezhdunarodnoi (Zvenigorodskoi) konferentsii po*

fizike plazmy i upravlyaemomy termoyadernomy sintezy (Abstracts of the 39th Int. (Zvenigorod) Conf. on Plasma Physics and Controlled Thermonuclear Fusion (Zvenigorod, IOFRAN, 2012) p. 220.
26. Ionin A.A., Kudryashov S.I., Levchenko A.O., et al. *Appl. Phys. Lett*., **100**, 104105 (2012).
27. Zvorykin V.D., Ionin A.A., Levchenko A.O., et al. *Kvantovaya Elektron*., **43** (4), 339 (2013) [*Quantum. Electron*., **43** (4), 339 (2013)].
28. Molchanov A.G. *Trudy Fiz. Inst. Akad. Nauk SSSR*, **171**, 54 (1986).
29. Tilleman M.M., Jacob J.H. *Appl. Phys. Lett*., **50**, 121 (1987).
30. Zvorykin V.D., Lebo I.G., Rozanov V.B. *Kratk. Soobshch. Fiz*., (9–10), 20 (1997).
31. Hooker C.J., Ross I.N., Shaw M.J. *Annual Rep. Rutherford Appleton Laboratory* RAL-87-041 (Chilton, UK, 1987) p. 226.
32. Tomie T., Okuda I., Yano M. *Appl. Phys. Lett*., **55**, 325 (1989).
33. Simon P., Gerhardt H. *Opt. Lett*., **14**, 1207 (1989).
34. Zvorykin V.D., Arlantsev S.V., Bakaev V.G., et al. *Proc. Conf. 'Inertial Fusion Sciences and Appl. 2003'* (Monteray, American Nuclear Society, Inc., 2004) pp 548–552.
35. Obenschain S.P., Colombant D.G., Schmitt A.J., et al. *Phys. Plasmas*, **13**, 056320 (2006).
36. Ewing J.J., Haas R.A., Swingle J.C., et al. *IEEE J. Quantum Electron*., **QE-15**, 368 (1979).
37. Lehmberg R.H., Giuliani J.L., Schmitt A.J. *J. Appl. Phys*., **106**, 023103 (2009).
38. Obenschain S.P., Sethian J.D., Schmitt A.J. *Fusion Sci. Techol*., **56**, 594 (2009).
39. Gus'kov S.Yu. *Fiz. Plazmy*, **39**, 3 (2013).
40. Kannari F., Obara M., Fujioka T. *J. Appl. Phys*., **57**, 4309 (1985).
41. Kannari F. *J. Appl. Phy*s., **67**, 3954 (1990).
42. Morgan W.L., Winter N.W., Kulander K.C. *J. Appl. Phys*., **54**, 4275 (1983).
43. Kvaran A., Shaw M.J., Simons J.P. *Appl. Phys. B*, **46**, 95 (1988).